International Journal of Engineering Sciences & Emerging Technologies, Dec. 2014.
ISSN: 2231 – 6604 Volume 7, Issue 3, pp: 658-679 ©IJESET

A NOVEL DESIGN OF UWB MONOPOLE ANTENNA AND ITS LINEAR ARRAYS

[1]Hosny El Metaafy, [2]Mahmoud Mohana, [3]Ali Gomaa, [4]Mamdouh Shaker Yacoub
[5]Gamal Kassem
[1]Higher Technological Institute 10th of Ramadan city (H.T.I)
[2]National Research Institute of Astronomy and geophysics (NRIAG)
[3]Faculty of Engineering, Shoubra, Benha University
[4]High Obour Institute, Obour City, Egypt
[5]Higher Technological Institute 10th of Ramadan city (H.T.I)

ABSTRACT

A novel design of ultra-wideband (UWB) monopole antenna is proposed with small size for UWB applications. An equivalent circuit for the proposed monopole antenna is obtained using the Advanced Design System (ADS). A parametric study for the major effective parameters of the antenna is done to study the effect of these parameters and get the optimized values of the antenna parameters. An UWB power divider circuit is designed to be used for exciting 2x1 and 4x1 linear antenna arrays to increase the antenna gain. The antenna element, UWB power divider and antenna arrays are simulated using CST-Microwave Studio and fabricated on FR-4 substrate with dielectric constant of 4.5 and thickness of 1.5 mm. The average gain for the two-element antenna array is about 5.3 dBi and reaches to7.15 dBi for the four-element antenna array, over the whole UWB frequency range. A good agreement between the measured and the simulated results for the antenna element, power divider and antenna arrays is appeared within the whole UWB frequency range.

KEYWORDS: *monopole antenna, Ultra-wide band, antenna array, power divider, stub matching.*

I. INTRODUCTION

Recently, the unlicensed Ultra-wideband (UWB) technology for commercial communications released by the Federal Communication Commission (FCC) is used in several applications. The concept of UWB radio was first developed several decades ago exactly in the late1960's. The U.S. Development of Defense first founded the term 'Ultra wideband' in 1989 [1]. In the beginning, UWB was mainly for military purposes such as radar applications which use wideband signals in frequency domain or very short duration pulses in the time domain to get fast, reliable and accurate information about moving targets such missiles. UWB technology has a great interest especially in 2002 since the US Federal Communication Commission (FCC) allowed the using of the unlicensed frequency band starting from 3.1 to 10.6 GHz for commercial communication applications [2]. The allocated FCC bandwidth is 7.5 GHz which represent 110% fractional bandwidth of the center frequency. Ultra wide band technology plays a paramount role in the development of modern wireless communication devices by transmitting videos, audios and other high bandwidth data between multiples of devices in the vicinity of 10 m or 30 ft, which covers the appliances used in home or office achieving high speed transfer, between 40 to 60 megabits per seconds and recently may reach up to 1 gigabits per second, low cost and low power consumption (0.5mW). The major applications for the UWB are the commercial communication systems, like vehicular radar systems, imaging systems such as ground-penetrating radar, wall-imaging systems, medical systems, and surveillance systems. Also, in Wireless Personal Area Networks (WPANs) environments, UWB technology is an excellent solution for the ultra-high-speed data services up to 500 Mbps. These speeds can be greatly increased by using

antenna arrays instead of single antenna element and different beam forming techniques. In order to design UWB antenna array, the power divider circuits are required. The most popular power divider is the Wilkinson power divider [3]. However, it operates only in a narrow bandwidth so; it is a serious problem for the UWB application. In order to achieve the bandwidth of UWB (3.1-10.6GHz), a three-section Wilkinson power divider has been reported, which increases the bandwidth [4]. Many efforts have been introduced to meet this challenge. One is to use a narrow rectangle slot to couple the wave from the input to output ports [5]. Also, adding open stubs can broaden the bandwidth. By placing one open stub at the center of each branch, the n^{th} harmonic component is suppressed [6]. Also, one can use additional transmission lines and open stubs to increase the bandwidth [7]. But both of them just reconstruct the circuit of the single-section Wilkinson power divider. Many UWB antennas have been reported in recent years [12-16]. Many UWB antenna arrays have been reported in recent years [17-20].

In this paper a novel design of ultra-wideband (UWB) monopole antenna is proposed to cover frequency range 2.49–14.42 GHz with small size for UWB applications. Section 2 discusses the parametric study of the major effective parameters of the antenna. Section 3 presents the configuration of the UWB antenna and its optimized parameters. Section 4 indicates the measured results of the proposed UWB antenna element compared with simulated one. Section 5 discusses the equivalent circuit of the proposed UWB antenna. Section 6 indicates the circuit layout and the design equations for the modified Wilkinson power divider. Section 7 presents the designs of the single and double stage modified Wilkinson power divider. Section 8 indicates the design of the two elements UWB linear antenna array with its feeding network circuit and the parametric study of the inter-element spacing to get the optimized distance in order to overcome the mutual coupling between them in addition its measured results. Section 9 shows the design of the four elements UWB antenna array and its measured results.

II. EFFECT OF DESIGN PARAMETERS

It has been shown in the simulation result that the operating band width of the proposed monopole antenna dependent on many effective parameters such as L_f, L_g, L_t, W_{t2},W_g, r, L_1, L_2, W_1,and W_2 as shown at Fig.1. A parametric study has been done for ten independent parameters and the dielectric substrate material and substrate height are kept constant at 4.5 and 1.5 mm respectively. The parametric study has been done utilizing the CST Microwave Studio 2011 – Transient solver [8]. The effect of each parameter individually where the other parameters are kept constant, on the matching of the antenna is presented in next section.

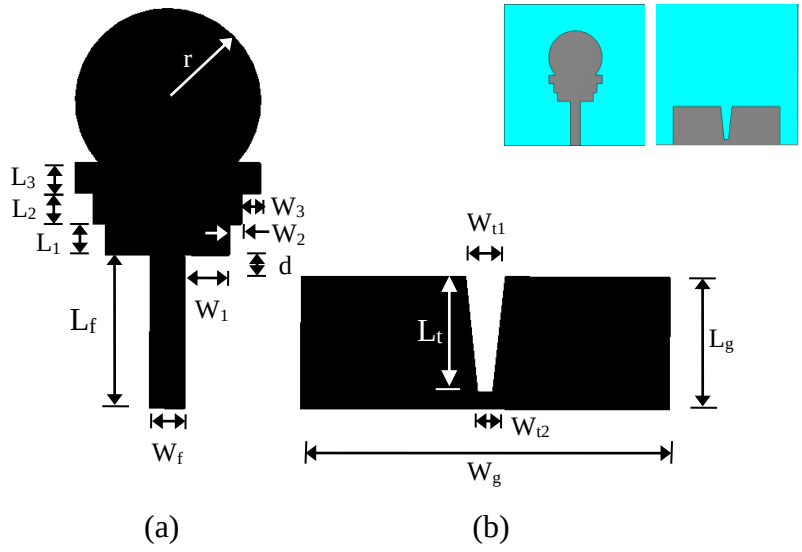

Fig.1. The geometry of the proposed UWB antenna structure:

(a) Patch layer (b) Ground plane layer.

2.1- Effect of the microstrip feed line (L_f).

Fig.2 shows investigation of the influence of the microstrip feed line (L_f) dimensions. Four values of the microstrip feed line (L_f) are assumed (11.5, 12.5, 13.5 and 14.5 mm). The values L_g, L_t, W_{t2},W_g, r, L_1, L_2, W_1,and W_2 are kept constant at 10.8 mm, 9.4 mm, 1.2 mm, 30 mm, 7.5 mm, 2.5 mm, 2.5 mm, 3.6 mm, and 1 mm respectively. It is clear that as the microstrip feed line (L_f) increases the impedance band width at the lower and upper resonant frequency bands decreased then it increased until we get the optimal value of L_f =12.5 mm.

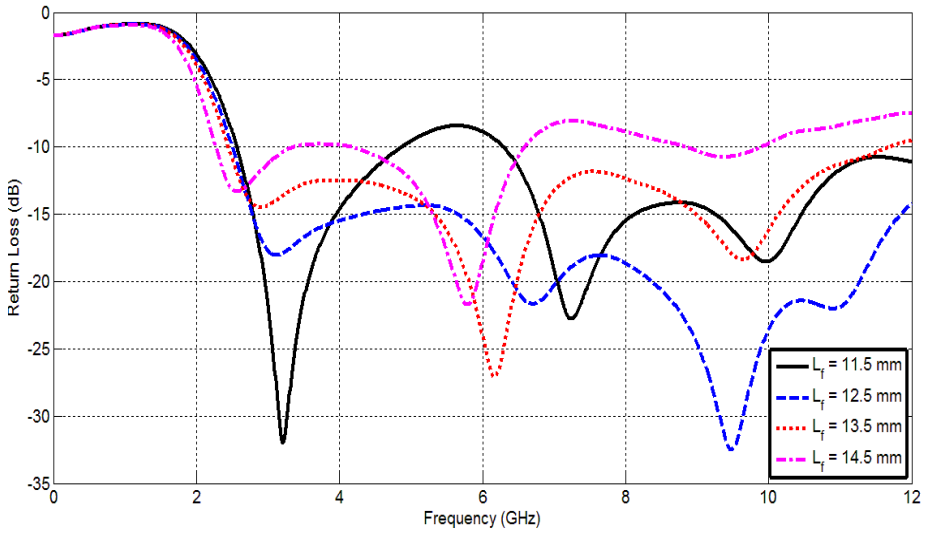

Fig.2 Parametric study of the microstrip feed line (L_f) dimensions.

2.2- Effect of the Ground plane length (Lg).

Fig.3 shows investigation of the influence of the ground plane length (L_g) dimensions. Three values of the ground plane length (L_g) are assumed (9.8, 10.8, and 11.8 mm). The values L_f, L_t, W_{t2},W_g, r, L_1, L_2, W_1,and W_2 are kept constant at 12.5 mm, 9.4 mm, 1.2 mm, 30 mm, 7.5 mm, 2.5 mm, 2.5 mm, 3.6 mm, and 1 mm respectively. It is clear from the Fig.3 that at the lower vales the ground plane length (L_g) a less matching occurred at the lower operating impedance band width while at the high /large vales the ground plane length (L_g) the less matching occurred at the shifted values of the operating impedance band width.

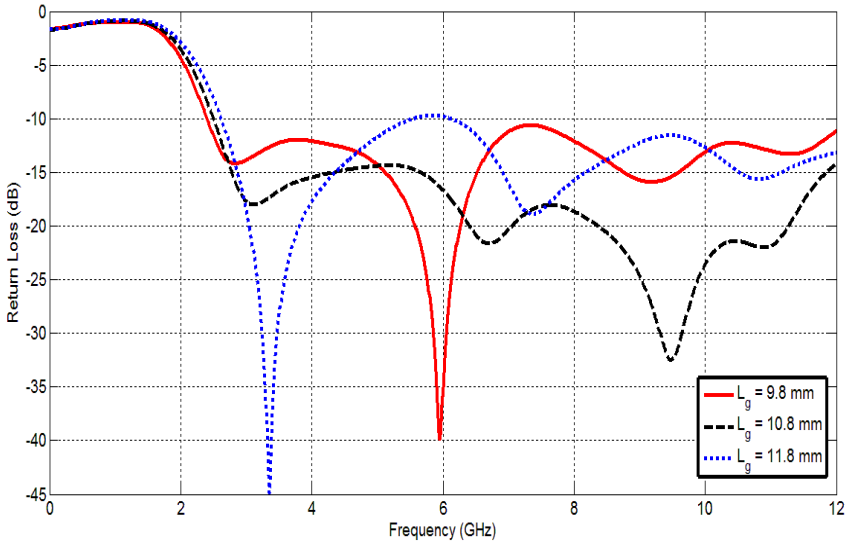

Fig.3 study of the ground plane length (L_g).

2.3- Effect of the length of the etched tapper (Lt) on the ground plane.

Fig.4 shows investigation of the influence of the length of the etched tapper (L_t) on the ground plane dimensions. Four values of the length of the etched tapper (L_t) on the ground plane are assumed (3.4, 5.4, 7.4, and 9.4mm). The values L_f, L_g, W_{t2},W_g, r, L_1, L_2, W_1,and W_2 are kept constant at 12.5 mm, 10.8 mm, 1.2 mm, 30 mm, 7.5 mm, 2.5 mm, 2.5 mm, 3.6 mm, and 1 mm respectively. It is clear from the Fig. 4 that as the length of the etched tapper (L_t) on the ground plane increases the matching of the impedance band width over the operating impedance band width increases.

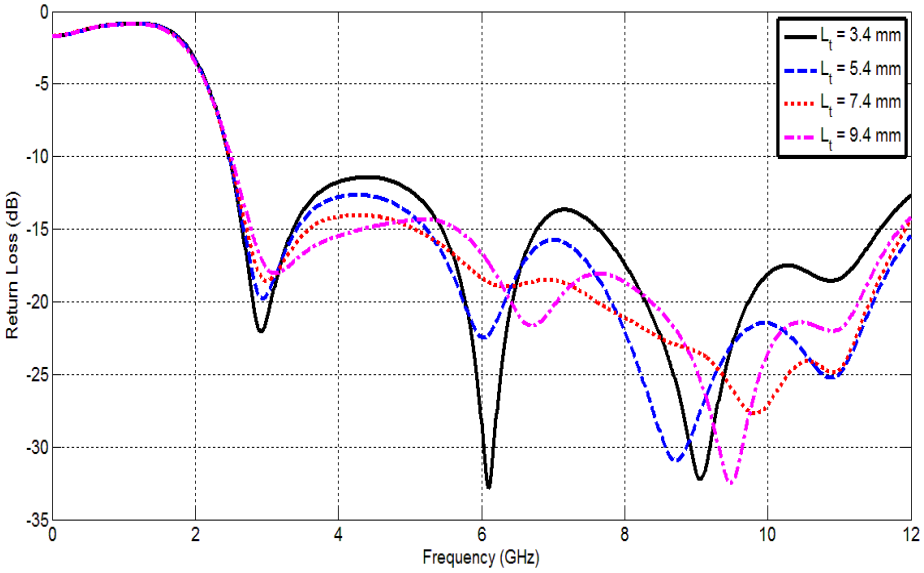

Fig.4 Parametric study of the length of the etched tapper (L_t) on the ground plane.

2.4- Effect of the bottom width of the etched tapper (Wt2) on the ground plane.

Fig.5 shows investigation of the influence of the bottom width of the etched tapper (W_{t2}) on the ground plane dimensions. Four values of the bottom width of the etched tapper (W_{t2}) on the ground plane are assumed (1.2, 1.6, 2.4, and 3.2 mm). The values L_f, L_g, L_t, W_g, r, L_1, L_2, W_1,and W_2 are kept constant at 12.5 mm, 10.8 mm, 9.4 mm, 30 mm, 7.5 mm, 2.5 mm, 2.5 mm, 3.6 mm, and 1 mm respectively. It is clear from the Fig.5 that as the bottom width of the etched tapper (W_{t2}) on the ground plane increases the matching of the impedance band width over the operating impedance band width decreases.

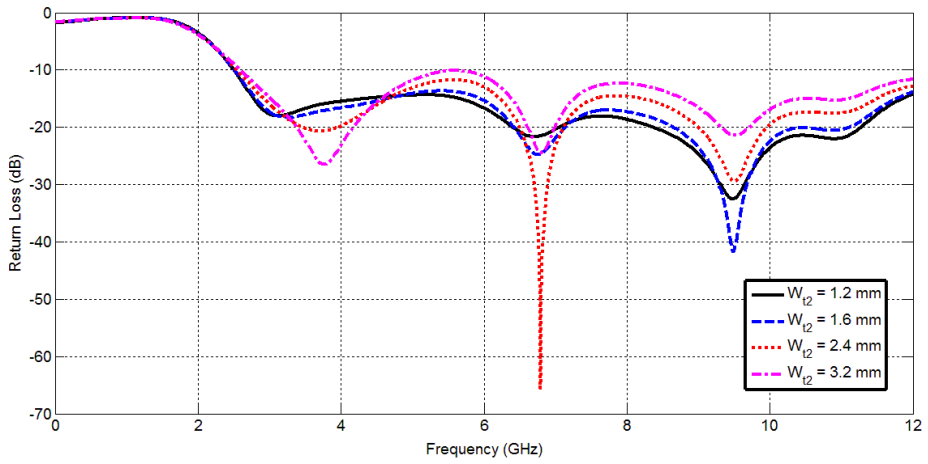

Fig.5 Parametric study of the bottom width of the etched tapper (W_{t2}) on the ground plane.

2.5- Effect of the width of the ground plane (Wg).

Fig.6 shows investigation of the influence of the width of the ground plane (W_g) dimensions. Four values of the width of the ground plane (W_g) are assumed (20, 25, 30, and 40 mm). The values L_f, L_g, L_t, W_{t2}, r, L_1, L_2, W_1,and W_2 are kept constant at 12.5 mm, 10.8 mm, 9.4 mm, 1.2 mm, 7.5 mm, 2.5 mm, 2.5 mm, 3.6 mm, and 1 mm respectively. It is clear from the Fig.6 that as the width of the ground plane increases the matching of the impedance band width over the operating impedance band width increases.

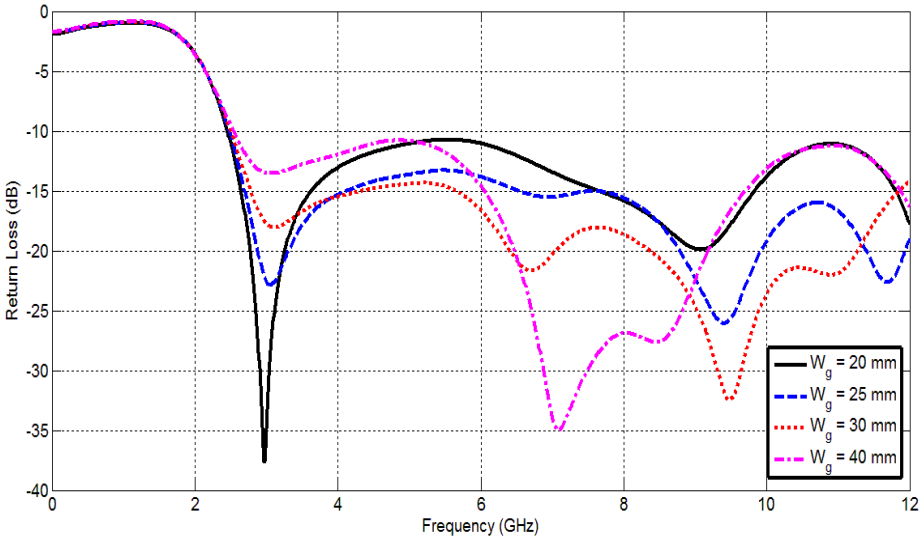

Fig.6 Parametric study of the ground plane width (W_g).

2.6- Effect of the radius of the circular patch antenna (r).

Fig.7 shows investigation of the influence of the radius of the circular patch antenna (r) dimensions. Four values of the radius of the circular patch antenna (r) are assumed (5.5, 6.5, 7.5, and 9.5 mm). The values L_f, L_g, L_t, W_{t2}, Wg, L_1, L_2, W_1,and W_2 are kept constant at 12.5 mm, 10.8 mm, 9.4 mm, 1.2 mm, 30 mm, 2.5 mm, 2.5 mm, 3.6 mm, and 1 mm respectively. It is clear from the Fig.7 that as the radius of the circular patch antenna (r) increases the matching of the impedance band width over the operating impedance band width increases then decreased.

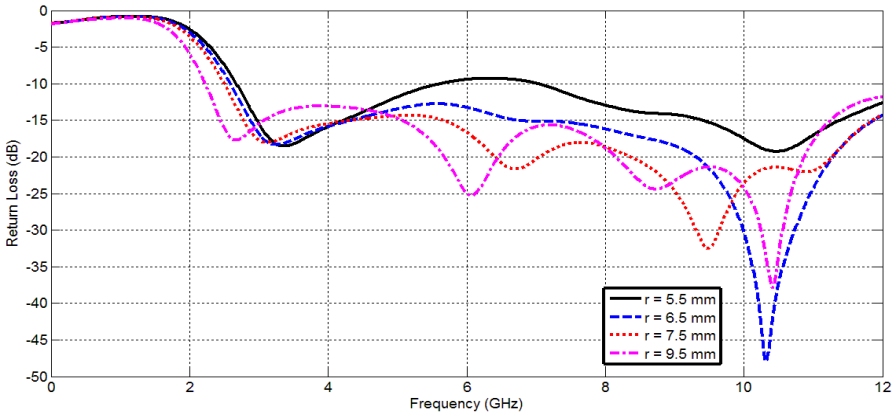

Fig.7 Parametric study of the radius of the circular patch antenna (r).

2.7- Effect of the first step length for the patch antenna (L1).

Fig.8 shows investigation of the influence of the first step length for the patch antenna (L_1) dimensions. Three values of the first step length for the patch antenna (L_1) are assumed (1.5, 2.5, and

3.5 mm). The values L_f, L_g, L_t, W_{t2}, Wg, r, L_2, W_1,and W_2 are kept constant at 12.5 mm, 10.8 mm, 9.4 mm, 1.2 mm, 30 mm, 7.5 mm, 2.5 mm, 3.6 mm, and 1 mm respectively. It is clear from the Fig.8 that as the first step length for the patch antenna (L_1) increases the matching of the impedance band width at the lower operating impedance band width decreases and increases at the upper operating impedance band width.

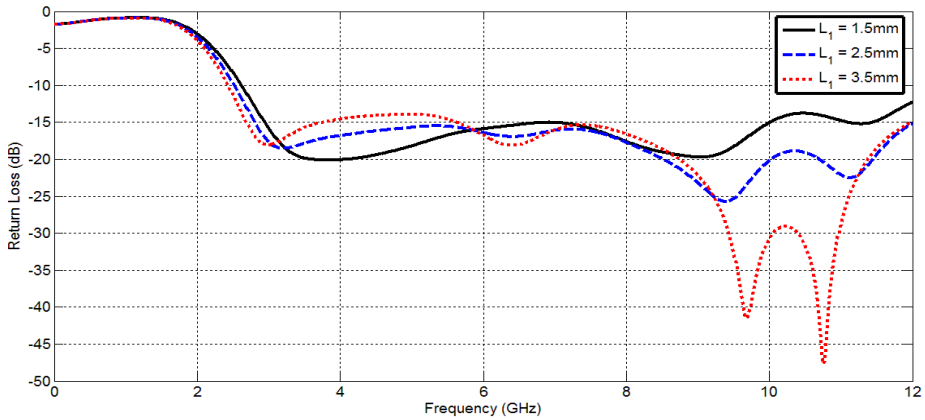

Fig.8 Parametric study of the radius of the first step length for the patch antenna (L_1)

2.8- Effect of the second step length for the patch antenna (L2).

Fig.9 shows investigation of the influence of the second step length for the patch antenna (L_2) dimensions. Three values of the second step length for the patch antenna (L_2) are assumed (1.5, 2.5, and 3.5 mm). The values L_f, L_g, L_t, W_{t2}, Wg, r, L_1, W_1,and W_2 are kept constant at 12.5 mm, 10.8 mm, 9.4 mm, 1.2 mm, 30 mm, 7.5 mm, 2.5 mm, 3.6 mm, and 1 mm respectively. It is clear from the Fig.9 that as the second step length for the patch antenna (L_2) increases the matching of the impedance band width at the lower operating impedance band width decreases and increases at the upper operating impedance band width.

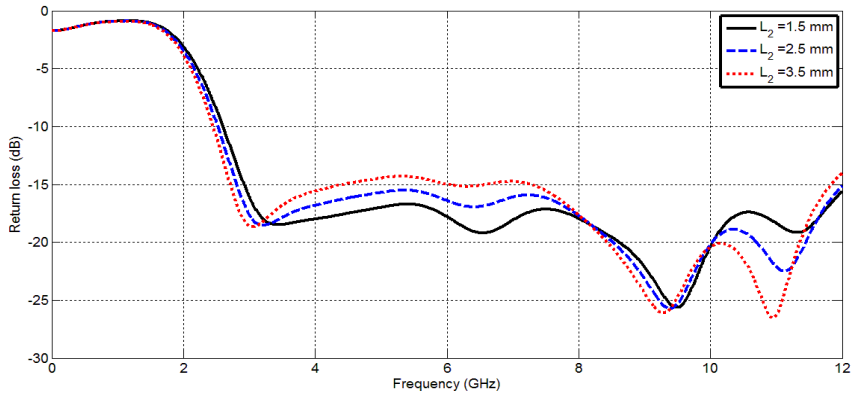

Fig.9 Parametric study of the radius of the second step length for the patch antenna (L_2)

2.9- Effect of the first step width for the patch antenna (W1).

Fig.10 shows investigation of the influence of the first step width for the patch antenna (W_1) dimensions. Four values of the first step width for the patch antenna (W_1) are assumed (1.6, 2.6, 3.6 and 4.6 mm). The values L_f, L_g, L_t, W_{t2}, Wg, r, L_1, L_2,and W_2 are kept constant at 12.5 mm, 10.8 mm, 9.4 mm, 1.2 mm, 30 mm, 7.5 mm, 2.5 mm, 2.5 mm, and 1 mm respectively. It is clear from the Fig.10 that as the first step width for the patch antenna (W_1) increases the matching of the impedance band width over all the operating impedance band width increases then it decreases at the center of the operating band width.

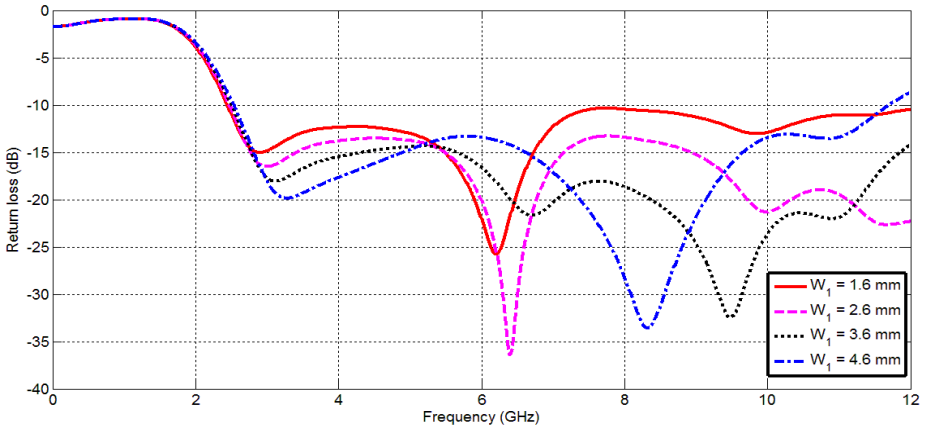

Fig.10 Parametric study of the radius of the first step width for the patch antenna (W_1)

2.10- Effect of the second step length for the patch antenna (W_2).

Fig.11 shows investigation of the influence of the second step width for the patch antenna (W_2) dimensions. Four values of the second step width for the patch antenna (W_2) are assumed (0.5, 1, 1.5, and 2 mm). The values L_f, L_g, L_t, W_{t2}, Wg, r, L_1, L_2,and W_1 are kept constant at 12.5 mm, 10.8 mm, 9.4 mm, 1.2 mm, 30 mm, 7.5 mm, 2.5 mm, 2.5 mm and 3.6 mm respectively. It is clear from the Fig.11 that as the second step width for the patch antenna (W_2) increases the matching of the impedance band width at the lower operating impedance band width increases and decreases at the upper operating impedance band width.

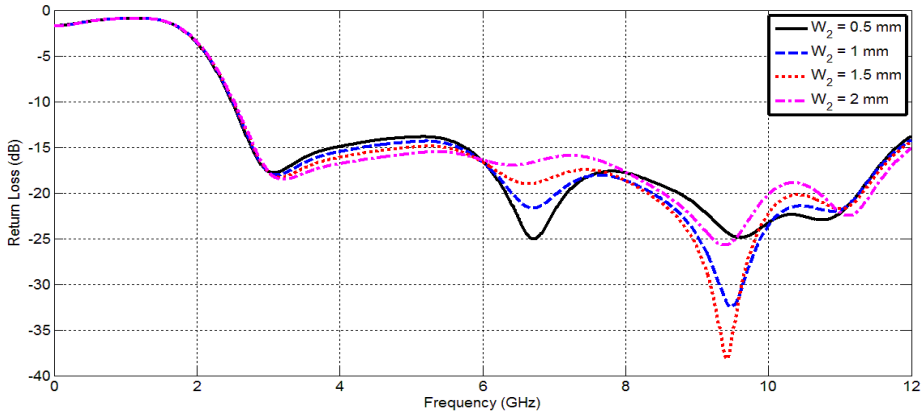

Fig.11 Parametric study of the radius of the second step width for the patch antenna (W_2)

III. UWB ANTENNA DESIGN AND CONFIGURATION

A novel design of UWB monopole microstrip antenna is proposed. A prototype of the proposed microstrip monopole antenna with optimal design parameters is shown in Fig. 12. The configuration of the proposed antenna consists of a circular patch with two steps, a partial ground plane with tapered trapezoidal defected ground structure (DGS), and a microstrip feed-line. The antenna structure is designed on FR4 substrate with dielectric constant of ε_r= 4.5, loss tangent 0.025 and substrate thickness of 1.5 mm. The antenna was simulated using CST Microwave studio 2011[8]. The optimized antenna parameters are shown in table 1.

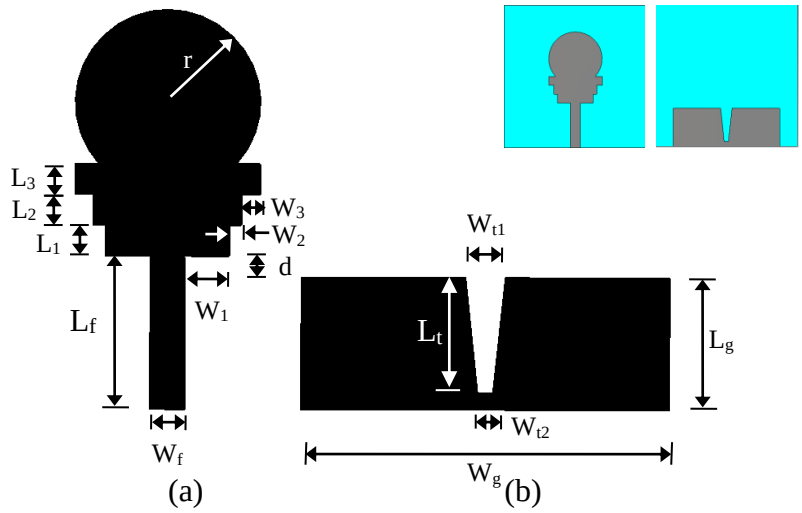

Fig.12. The geometry of the proposed UWB antenna structure:

(a) Patch layer (b) Ground plane layer.

Table 1 The optimized parameters for the proposed UWB antenna.

Parameter	Value (mm)	Parameter	Value (mm)	Parameter	Value (mm)
L_g	10.8	L_2	2.5	d	1.7
W_g	30	L_3	2.5	W_{t1}	3.2
L_f	12.5	W_1	3.6	W_{t2}	1.2
W_f	2.8	W_2	1	r	7.5
L_1	2.5	W_3	1.5	L_t	9.4

IV. RESULTS AND DISCUSIONS

The proposed antenna was designed using CST Microwave studio software package, which utilizes the finite integration technique for electromagnetic computation. Fig. 13 shows the measured and simulated return loss of the proposed antenna.

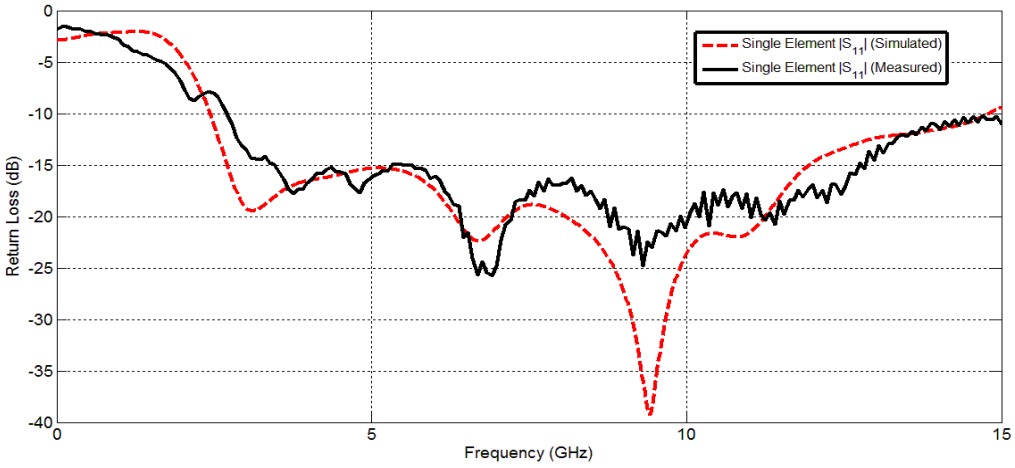

Fig. 13. The measured and simulated return loss of the proposed monopole antenna**.**

The simulated 10-dB return loss bandwidth is from 2.49 GHz to 14.42 GHz and is from 2.69 GHz to 14.93 GHz for the measured one. The simulated gain and directivity curve versus the frequency is shown in Fig. 14. It is seen that the gain has a good level through the high frequency band. Fig. 15 and

Fig. 16 show the measured and simulated far-field radiation pattern (E-plane and H-plane) for the proposed antenna at frequencies 3.1GHz and 5 GHz respectively. Fig. 17 shows the photos of the fabricated antenna connected with the vector network analyzer R&S Model (ZVB20).

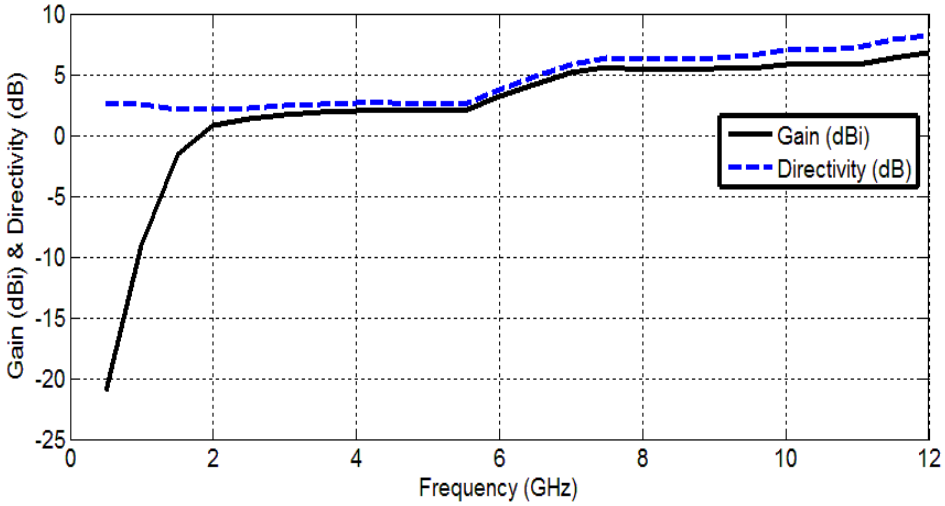

Fig. 14. The simulated gain and directivity versus the frequency.

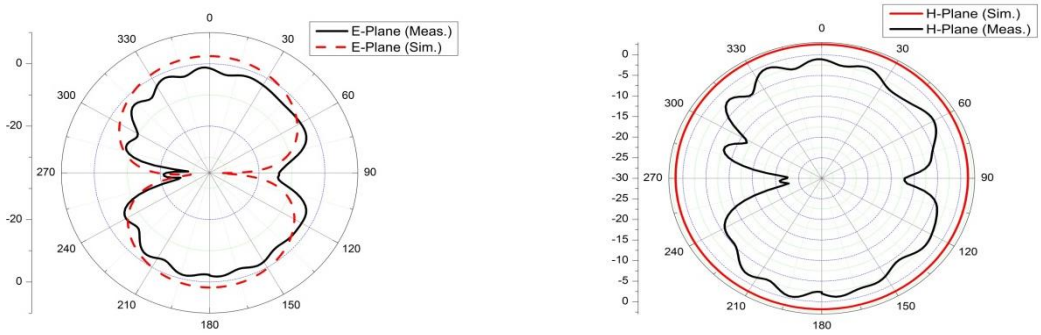

E-plane H-plane

Fig. 15. The measured and simulated far-field radiation pattern at frequency 3.3GHz.

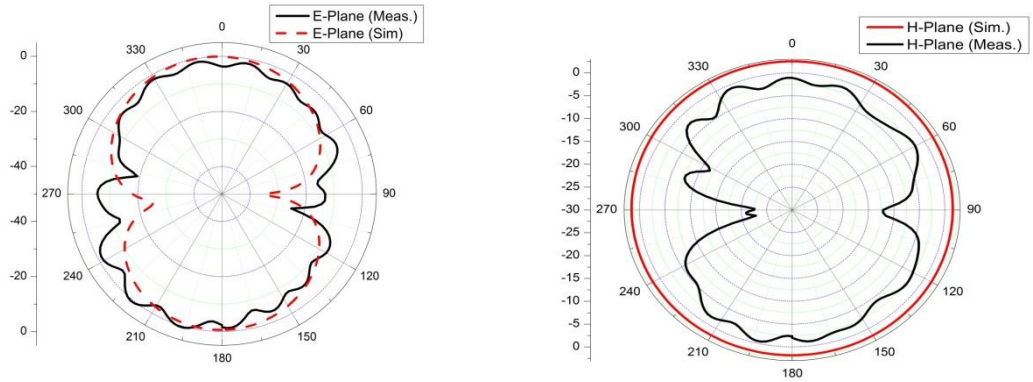

E-plane H-plane

Fig. 16. The measured and simulated far-field radiation pattern at frequency 5 GHz.

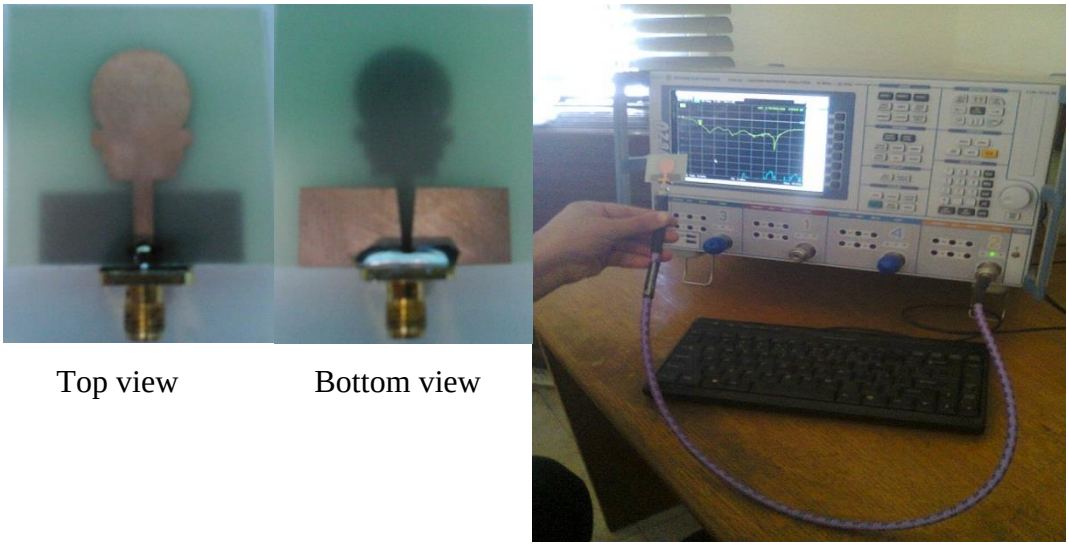

Top view Bottom view

Fig. 17. The fabricated photos of the proposed UWB antenna

V. UWB ANTENNA EQUIVALENT CIRCUIT

A simplified lumped element circuit model of the UWB patch antenna has been proposed. This model was obtained by studying the scattering parameter (S_{11}) of the antenna structure by simulating the antenna in CST Microwave Studio. By obtaining this S-parameter the overall structure of the circuit model had been transformed to imply the characteristics of the antenna. The equivalent circuit of patch antenna is shown in Fig. 18 where patch cavity is modeled as a parallel RLC circuit, while the probe inductance is modeled as a series inductor. Fig. 19(a) shows the structure of step discontinuity. The equivalent circuit of the unit of step discontinuity is modeled as Fig. 19(b).

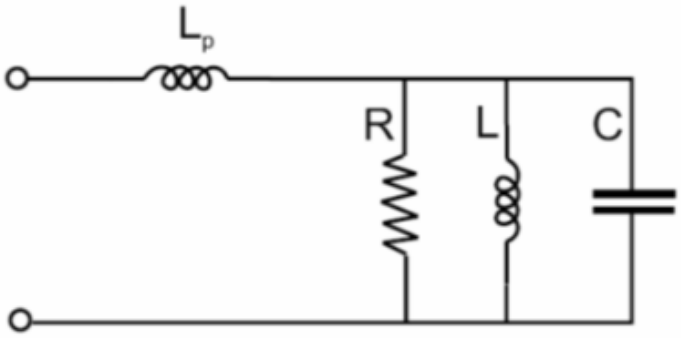

Fig. 18 . Equivalent circuit of patch antenna.

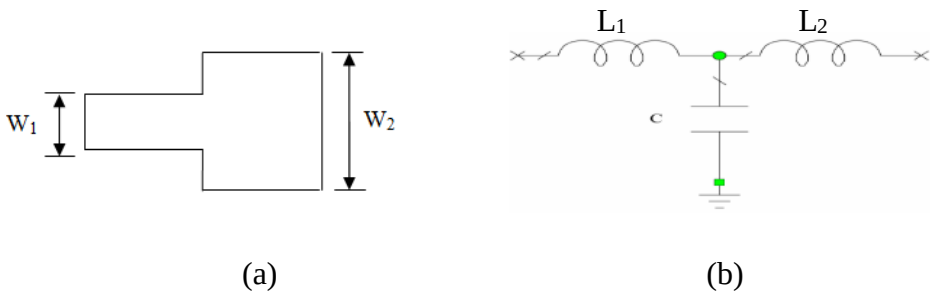

(a) (b)

Fig. 19 (a) Structure of step discontinuity (b) The equivalent circuit of the unit of step discontinuity

Fig. 20 shows the equivalent circuit of UWB circular patch antenna. The proposed antenna is designed by using equivalent circuit of step discontinuity, circular patch antenna. In this model the patch is modeled as a parallel RLC circuit. The circuit model had been simulated using Advanced Design System 2008 (ADS) simulator and the S-parameter is compared with the obtained scattering parameter from simulating the EM structure in CST microwave studio simulator. Fig.21 shows a simulated return loss of the UWB patch antenna compared with the circuit simulator model. Table 2 shows the optimized parameters for the equivalent circuit model of the proposed UWB antenna.

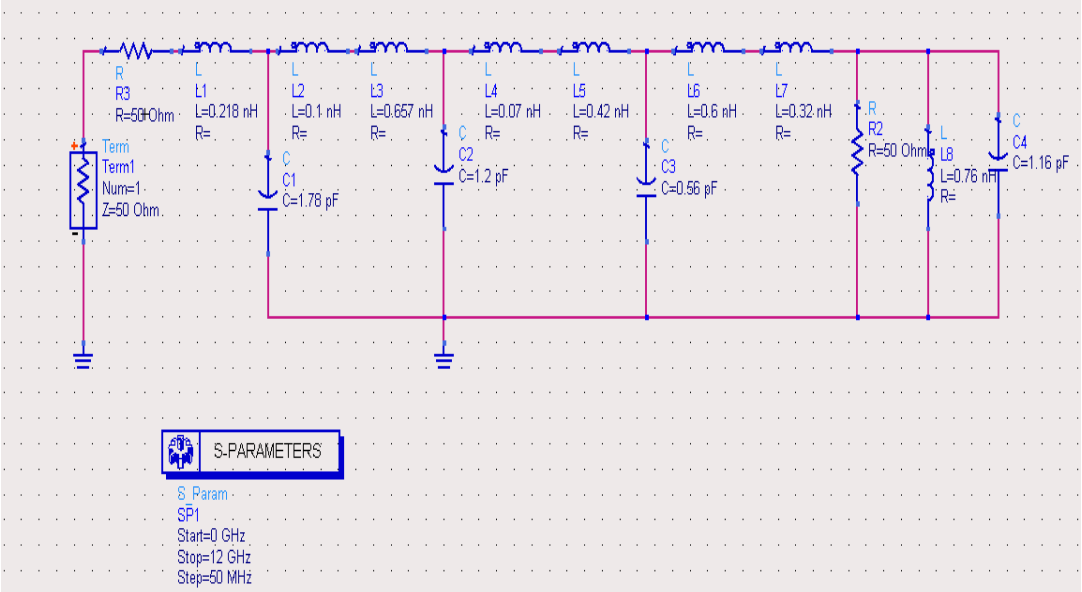

Fig. 20. The equivalent circuit of UWB circular proposed patch antenna

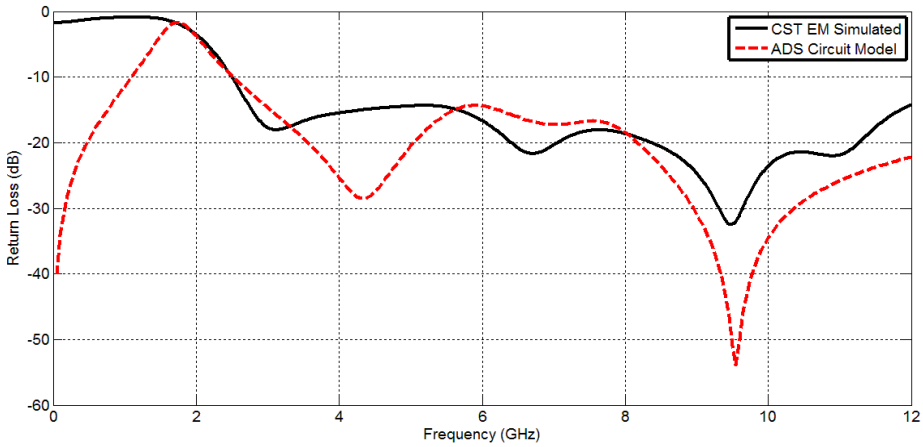

Fig. 21. Simulated return loss of the proposed antenna compared with the circuit simulator model.

Table 2 The optimized parameters for the circuit model of the proposed UWB antenna.

Parameter	Value (nH)	Parameter	Value (nH)	Parameter	Value (pF)
L_1	0.218	L_5	0.42	C_1	1.78
L_2	0.1	L_6	0.6	C_2	1.2
L_3	0.657	L_7	0.32	C_3	0.56
L_4	0.07	L_8	0.76	C_4	1.16

VI. MODIFIED WILKINSON POWER DIVIDER

The design of UWB feeding networks is based on modifying the traditional Wilkinson power divider. Fig. 22 shows the circuit layout of the feeding network for UWB operation [10]. As shown from Fig.

22, it composed of a modified one- section Wilkinson power divider which has characteristic impedance of Z_1 and electrical length θ_1. For broadening the bandwidth a stub matching network is added to each branch with additional transmission line at the end of the stage. By other word, an extended transmission line with parameters (Z_1, θ_1') and an open circuit stub (OC) with parameters (Z_s, θ_s) have been added to each branch. The two aforementioned sections are connected to another section of Wilkinson power divider with transmission line of (Z_2, θ_2) at the end of the stub matching network. By adjusting the length and width of the OC stubs, the bandwidth can be broadened.

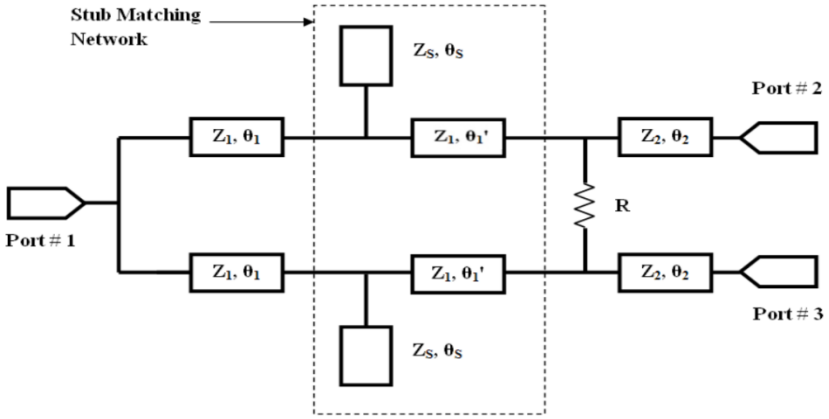

Fig. 22. The circuit layout of the proposed feeding network for UWB operation [10].

First, a conventional Wilkinson power divider is designed with its center frequency f_0 = 6.85 GHz and bandwidth ratio (f_U/f_L) equal 3.42 for covering the whole UWB frequency range (3.1-10.6 GHz). It is shown from Fig. 22 that it consists of a modified two-section Wilkinson power divider in [8] with removing the resistor of the second section R_2. The input and output impedance are chosen to be 50 Ω. Only one resistor is placed between the output ports to prevent the signal transmission and obtain a good isolation between them. According to the desired bandwidth ratio ($m = f_U/f_L$) the initial values for the divider parameters Z_1, θ_1, Z_2, θ_2 and B_s can be determined by means of elementary transmission line theory [9]. Then the length of the extended line is chosen arbitrarily to be different than that of the main line ($\theta_1' \neq \theta_1$) to obtain more flexibility and degree of freedom and hence the bandwidth can be enhanced. In order to get the values of Z_1, Z_2, Z_s, θ_1, θ_2, θ_1' and B_s an even mode and odd mode analysis is derived in [4, 9, 10] with removing the resistor of the second section R_2 using equations (1-5). The initial value of θ_1 can be calculated according to the operating bandwidth from equation (1) [9]:

$$\theta_1 = 90^o \left[1 - \frac{1}{\sqrt{2}}\left(\frac{f_u/f_l - 1}{f_u/f_l + 1}\right)\right] \quad (1)$$

$$Z_2 = Z_0 \sqrt{\frac{1}{2\alpha} + \sqrt{\frac{1}{4\alpha^2} + 2}} \quad (2)$$

$$Z_1 = \frac{2 Z_0^2}{Z_2} \quad (3)$$

$$\alpha = (\tan(\theta_1)^2 = \left[tan\left(\beta_1 \cdot \frac{n\pi}{\beta_1(1+m)}\right)\right]^2 = \left[tan\left(\frac{n\pi}{(1+m)}\right)\right]^2$$

n = 1 the frequency ratio between (1 < m < 3)

$$B_s = \left(1 - tan(\theta_1)\, tan(\theta_1')\right)/(Z_1 tan(\theta_1)) = tan\theta_s/Z_s \quad (4)$$

$$Z_s = \left(Z_1 tan(\theta_1)\, tan(\theta_s)\right)/\left(1 - tan(\theta_1)\, tan(\theta_1')\right) \quad (5)$$

VII. SINGLE AND DOUBLE STAGE MODIFIED WILKINSON POWER DIVIDER

The initial investigations of the proposed UWB feed network parameters were made from summarized table 3. The proposed UWB feed network is designed on FR4 substrate with dielectric substrate ε_r =4.5 and substrate height =1.5 mm. The overall size of proposed UWB feed network is 23 x 19.5 mm^2. The parameters of the proposed feed network were optimized using IE3D Zeland ver. 12 to obtain a good reflection coefficient at all ports and good isolation over the whole UWB frequency

range. The final dimension of the optimized parameters for the proposed feeding network is summarized in table 4.

Table 3 The initial parameters of the proposed UWB feed network

Parameter	Z_1	θ_1	θ_1'	Z_2	θ_2	Z_s	θ_s
Value	89 Ω	48.76°	27.1°	61 Ω	137°	52.1 Ω	11.2°

Table 4 The optimized parameters of the proposed UWB feeding network.

Parameter	W_1	L_1	L_1'	W_2	L_2	W_s	L_s
Value(mm)	0.67	2.18	2.015	1.98	10.12	2.63	0.55

The measured and simulated return loss at the input port (S_{11}) in addition to, the isolation between the output ports (S_{23}) for the proposed feed network are shown in Fig. 23. Fig. 24 shows the measured and simulated power division ratio at the output ports (S_{21}, S_{31}). The return loss at the input port is reaches to -40.45 dB at the middle of the interesting band and it reaches to 11.5 dB at the end of the band. The return losses at the output ports reach to-12.5 dB at the frequency 8 GHz and reaches to -40 dB at the end of the band. It can be seen that the power is divided equally between the output ports. The isolation between the two outputs ports (S_{23} =S_{32}) better than 12.8 dB at the start of the interesting band (3.1 GHz) and better than 15.8 dB throughout the other frequency range.

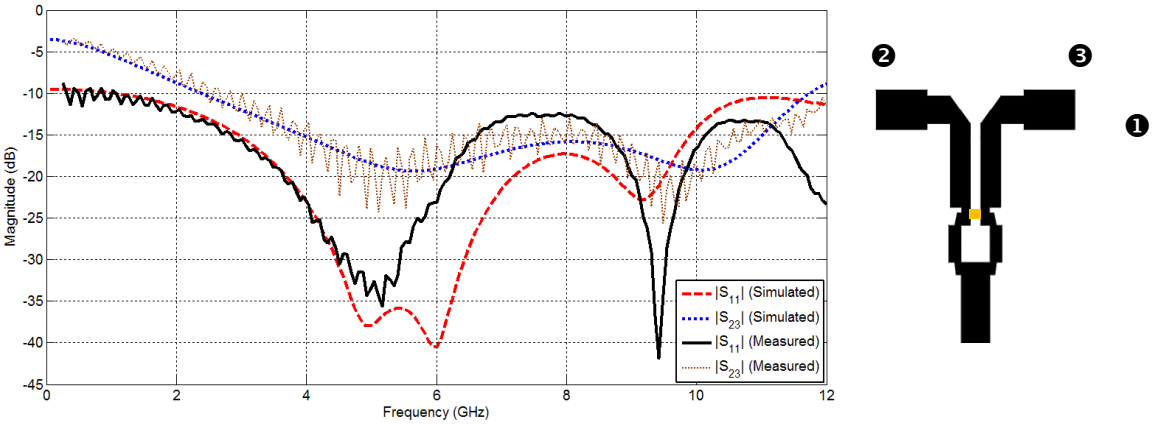

Fig. 23. The measured and simulated return loss at the input port (S_{11}) and the isolation between the output ports (S_{23}).

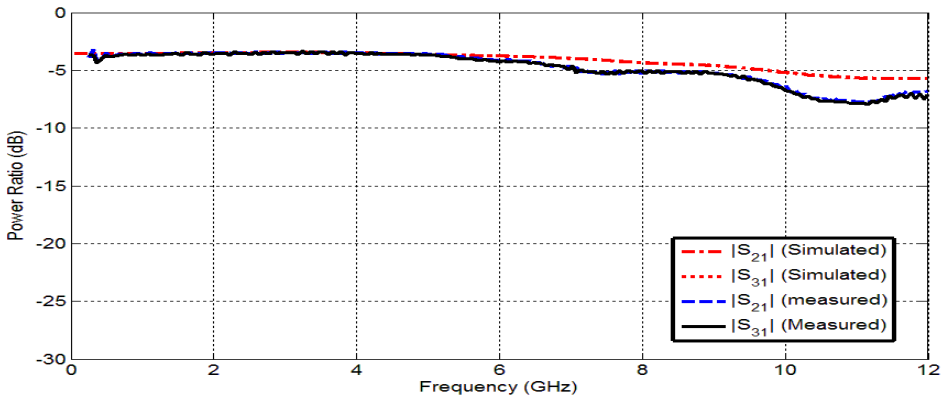

Fig. 24. The measured and simulated power ratio at the output ports (S_{21}, S_{31}).

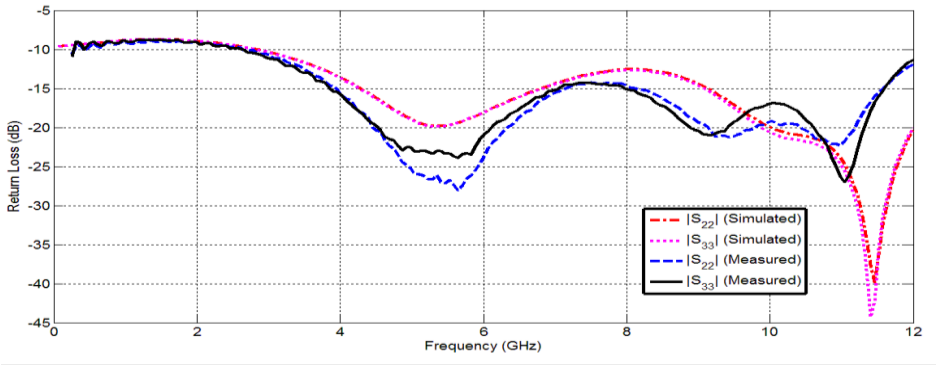

Fig. 25. The measured and simulated return loss at the output ports (S_{22}, S_{33}).

As shown from Fig. 24 the values of measured and simulated power ratio at the output ports (S_{21} and S_{31}) are equal at the same frequency over the all range of frequencies. However, these values (S_{21} and S_{31}) at the start of frequency range are different from that at the end of frequency range due to the use of FR4 material where the losses increased with the increase the frequency. Fig. 25 shows the measured and simulated return loss at the output ports (S_{22}, S_{33}).

Two Cascaded Modified Wilkinson power Divider is shown in Fig. 26. The two cascaded modified WPD are used to excite 4x1 linear UWB antenna array. The separating distance (d_1 = 35 mm) between the each adjacent output port is assigned to suitable to connect with the input microstrip transmission line of the UWB antenna array. The simulated return loss at the input port (S_{11}) and the isolation between the output ports (S_{23}, S_{34}, S_{45}) for the two cascaded modified Wilkinson power divider are shown in Fig. 27. Fig. 28 shows the simulated return loss at the output ports (S_{22}, S_{33}, S_{44}, and S_{55}) for two cascaded modified Wilkinson power divider. Fig. 29 shows the power ratios at the output ports (S_{21}, S_{31}, S_{41}, and S_{51}) for two cascaded modified Wilkinson power divider. Also, , the difference between values of power ratios at the output ports (S_{21}, S_{31}, S_{41}, and S_{51}) at the start of frequency range than that at the end of frequency range due to the use of FR4 material where the losses increased with the increase the frequency.

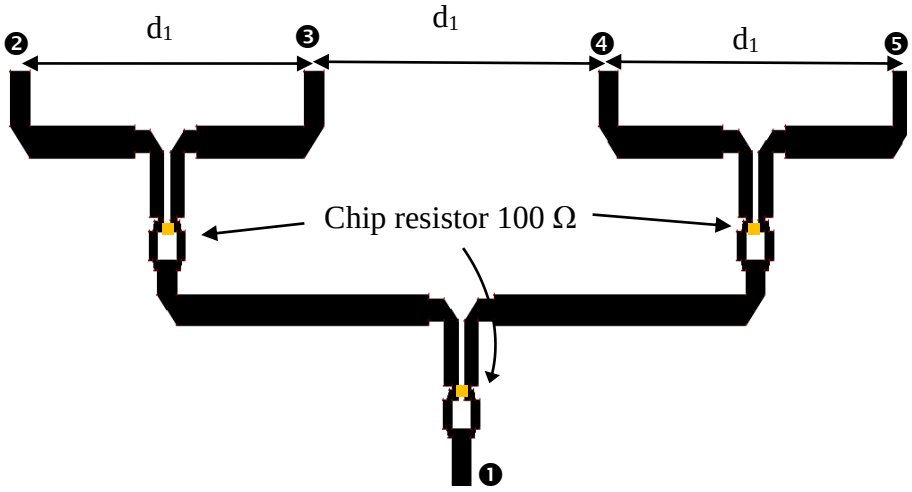

Fig. 26. Two Cascaded Modified Wilkinson power Divider

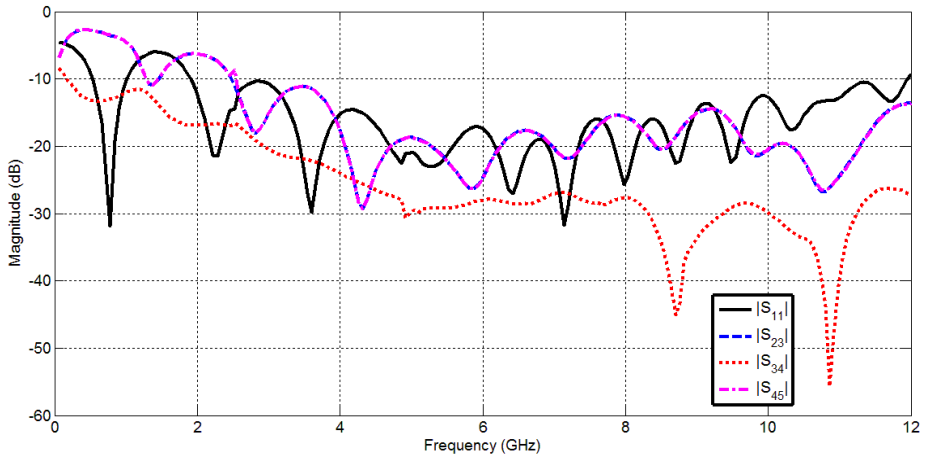

Fig. 27. The simulated return loss at the input (S_{11}) and the isolation between the output ports (S_{23}, S_{34}, S_{45}) for two cascaded modified Wilkinson power divider.

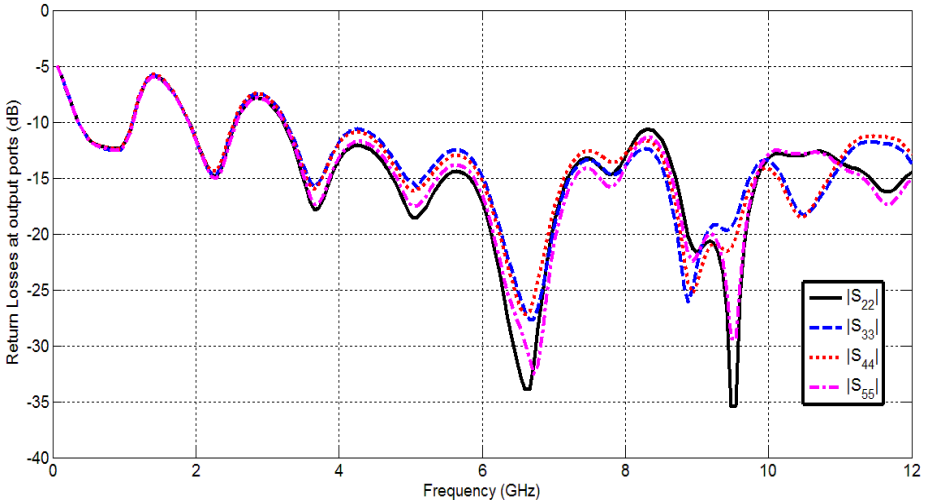

Fig. 28. The simulated return loss at the output ports (S_{22}, S_{33}, S_{44}, and S_{55}) for two cascaded modified Wilkinson power divider.

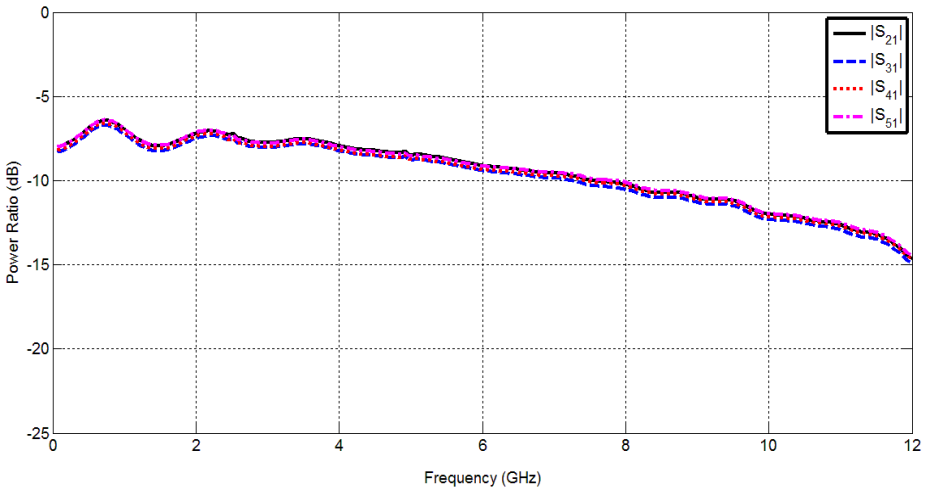

Fig. 29. The simulated power ratios at the output ports (S_{21}, S_{31}, S_{41}, S_{51}) for two cascaded modified Wilkinson power divider.

VIII. TWO ELEMENT ULTRA-WIDE BAND LINEAR ANTENNA ARRAY

The two-element UWB linear antenna arrays is composed of UWB feed network circuit which is previously designed and two UWB antenna elements. The geometry of the proposed two-element linear antenna array prototypes is shown in Fig. 30. The spacing between the antenna elements has a great effect on the overall performance of the array where the optimized value is 35 mm. Two UWB antennas without power divider circuit have been studied in order to show the effect of the distance between the antennas. Fig. 31 (a-c) shows the simulated return loss at the input of the two antennas and the coupling between the antenna elements. The target here is to design a two-element linear antenna arrays with good impedance matching characteristics across the desired UWB frequency range. Moreover, the designed arrays should obtain higher gain, and stable radiation patterns throughout the desired frequency band of interest. It has been found from the parametric studies that using a rectangular cut in the common ground plane of dimensions (W_g and L_g) in the two-element antenna array, the impedance matching of the antenna array is enhanced through the UWB frequency range. This rectangular cut reduces the mutual coupling between the two antenna elements. The optimized values for the rectangular cut in the common ground plane are: W_g= 5 mm and L_g = 10.8 mm. The interspacing distance between the two antenna effects on the impedance matching characteristic of the antenna and the grating lobe. The larger inter-element spacing, the higher grating lobe will be occurred. The smaller inter-element spacing, the mutual coupling between the two elements is increased as shown in Fig. 20. In case of d_1=30 mm the two ground planes of the two adjacent antennas are stuck (no rectangular cut between the two ground planes) which is cause the coupling between them.

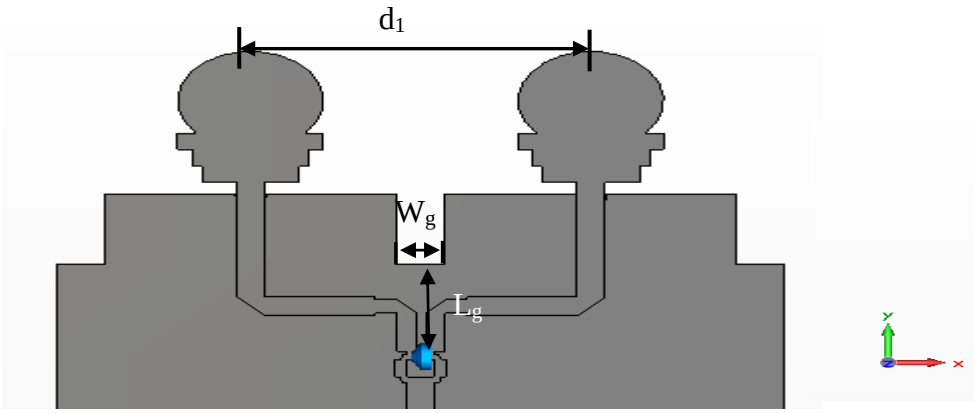

Fig. 30. The geometry of the proposed two-element linear antenna array prototypes

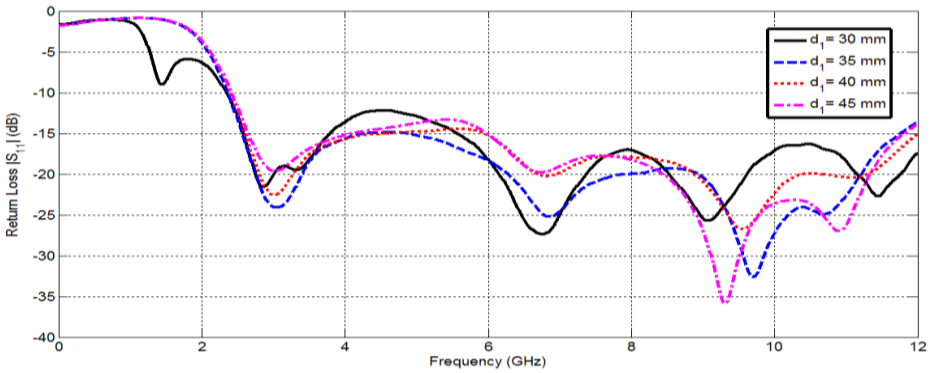

(a)

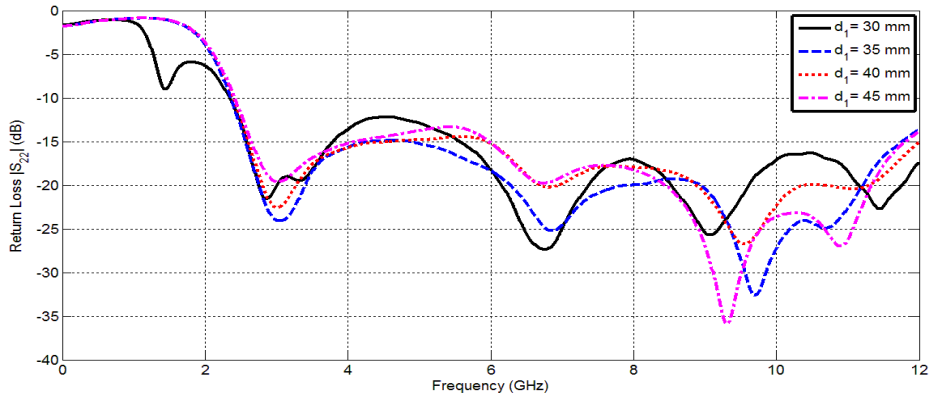

(b)

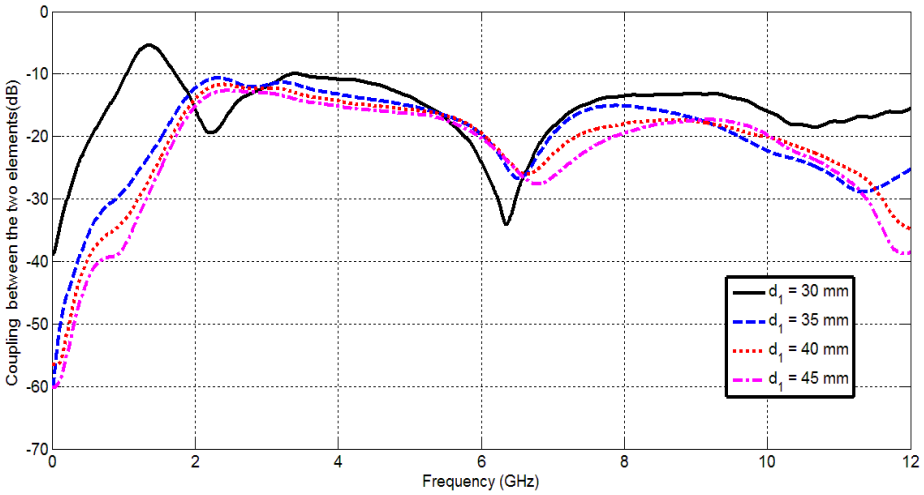

(c)

Fig. 31. The simulated return losses at the two antenna input ports: (a) S_{11} and (b) S_{22} (c) The coupling between the two antenna elements at different distance values (S_{21}).

The measured and simulated return loss curve for two elements antenna array connected with its power divider circuit are shown in Fig. 32. Fig. 33 shows the gain and the directivity curves over the interesting bands of frequency. Fig. 34 shows the measured and simulated far-field radiation pattern (E- plane and H-plane) at different values of frequency (3.3 GHz and 5 GHz). The matching at frequency equal 3.3 GHz is -11 dB and at frequency 5 GHz is -35 dB.

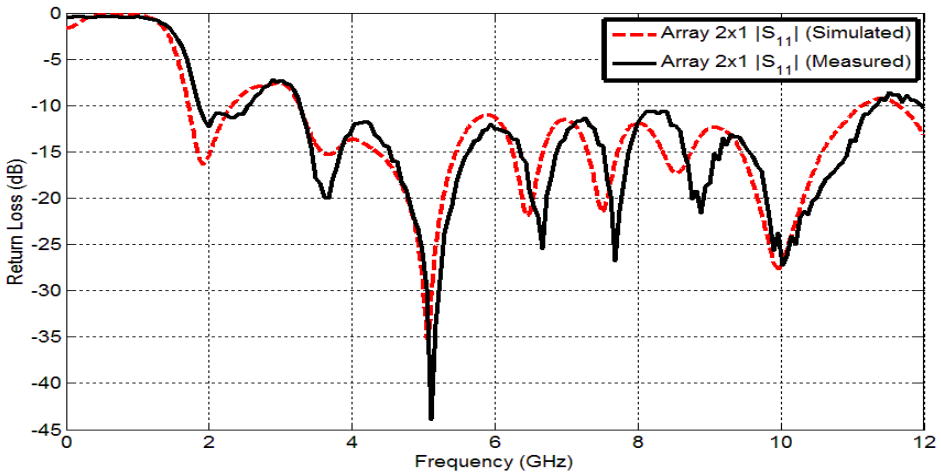

Fig. 32. The measured and simulated return loss for two elements antenna array connected with its power divider circuit.

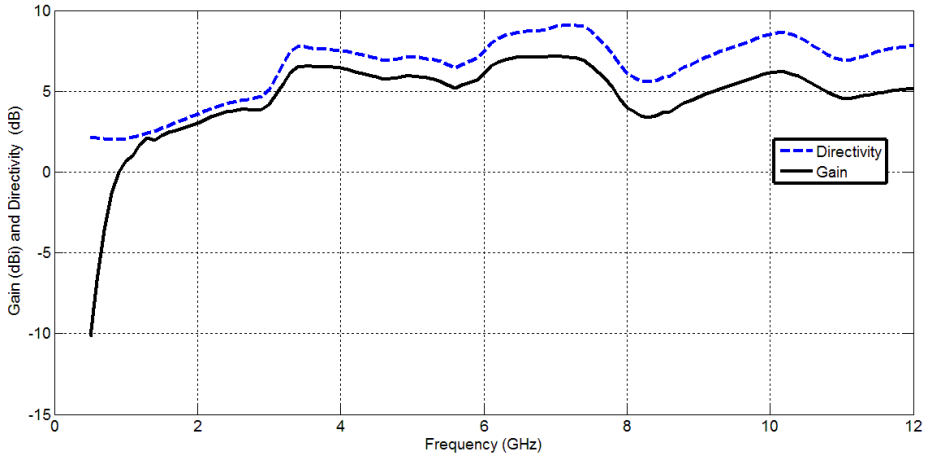

Fig. 33. The simulated gain and the directivity curves over the UWB frequency range.

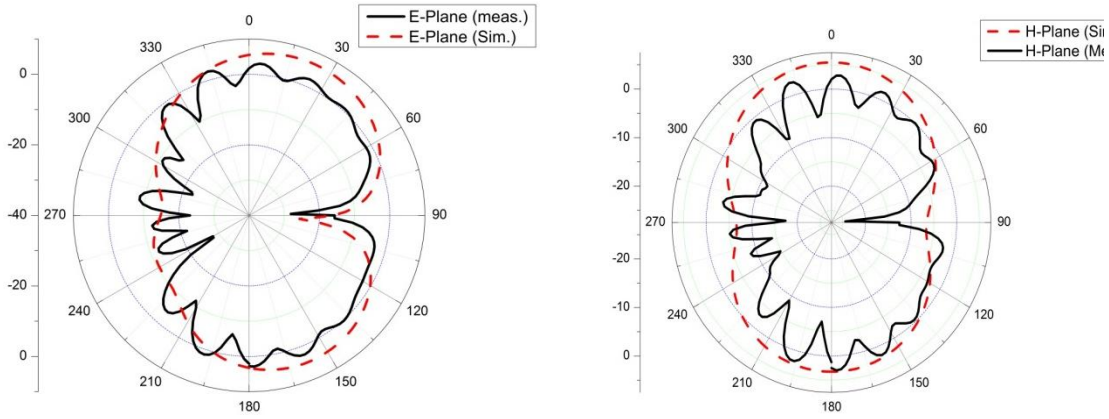

E-plane H-plane

(a)

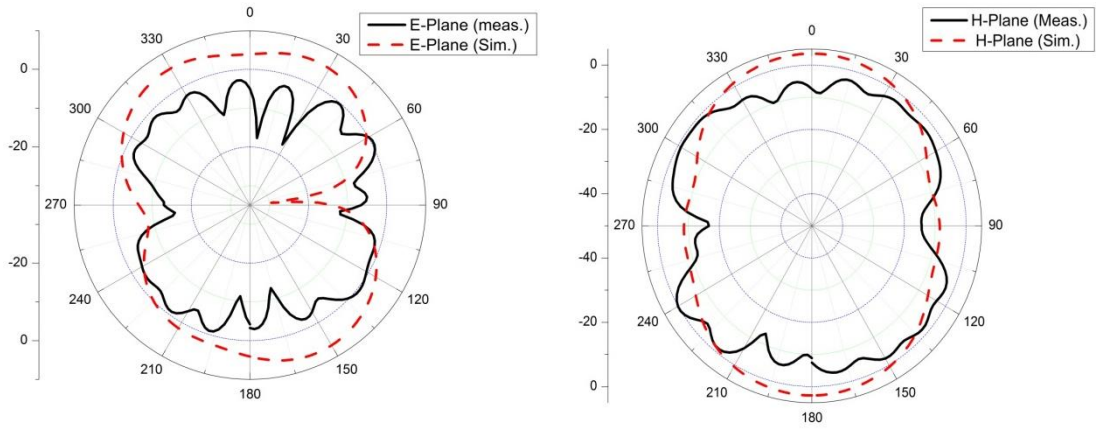

E-plane H-plane

(b)

Fig. 34. The measured and simulated far-field radiation pattern (E- and H-planes) at:
(a) f = 3.3 GHz (b) f = 5 GHz.

IX. FOUR ELEMENTS ULTRA-WIDE BAND ANTENNA ARRAY

The four-element UWB linear antenna arrays is composed of UWB feed network circuit which is previously designed and four UWB antenna elements. The geometry of the proposed four-element linear antenna array prototypes is shown in Fig. 35. The target is to design four-element linear antenna arrays with good impedance matching characteristics across the desired UWB frequency range.

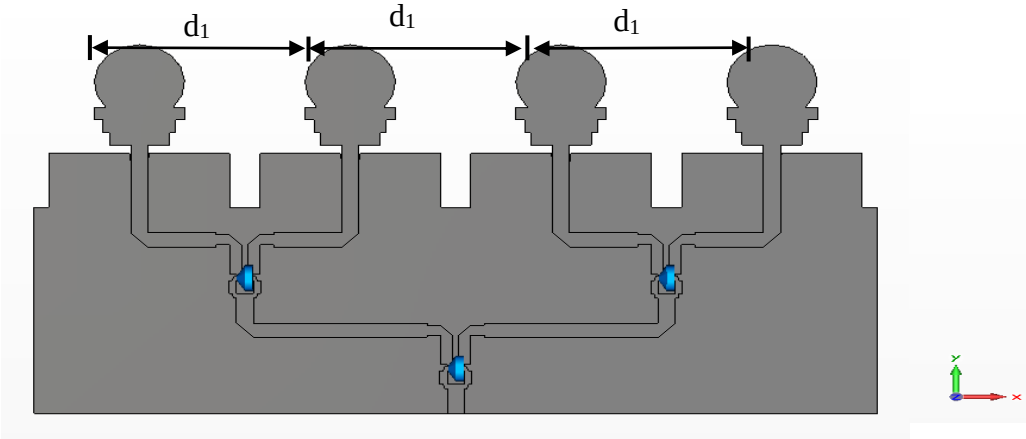

Fig. 35. The geometry of the proposed four-element linear antenna array prototypes.

The measured and simulated return loss for four elements antenna array connected with its power divider circuit is shown in Fig. 36. Fig. 37 shows the gain and the directivity curves over the interesting bands of frequency where the target of using array is to increase the gain. Fig. 38 shows the measured and simulated far-field radiation pattern (E- plane and H-plane) at different values of frequency. It is clear from Fig. 26 that the beam is more directive in the plane where the linear array is placed (Phi=0). Fig. 39 shows the fabricated photos of the proposed 4 x1 UWB linear antenna array.

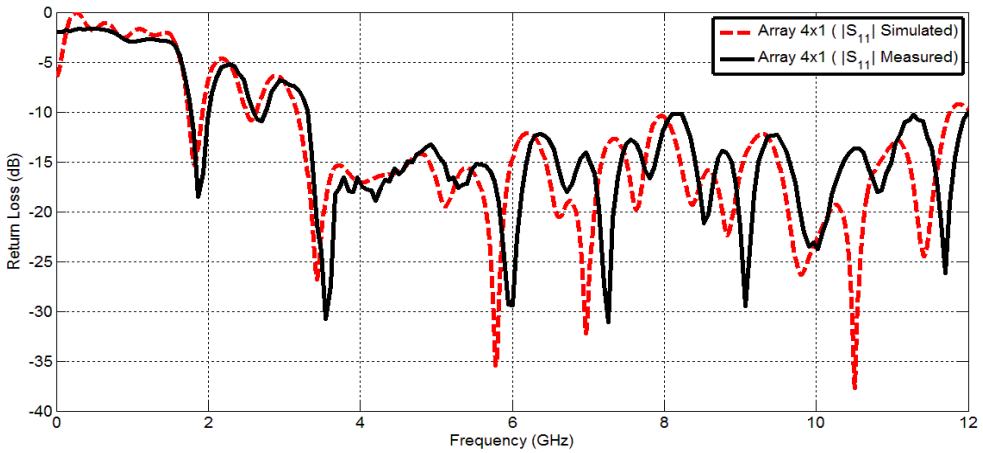

Fig. 36. The measured and simulated return loss for four elements antenna array connected with its power divider circuit.

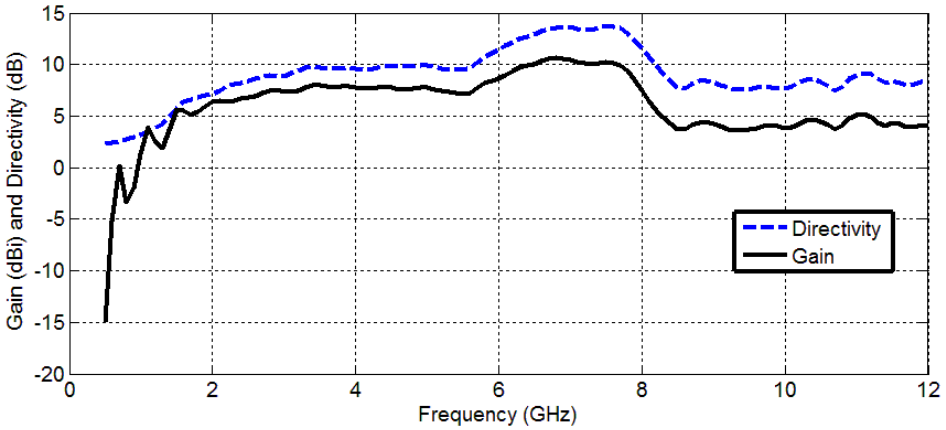

Fig. 37. The simulated gain and the directivity curves over the UWB frequency range.

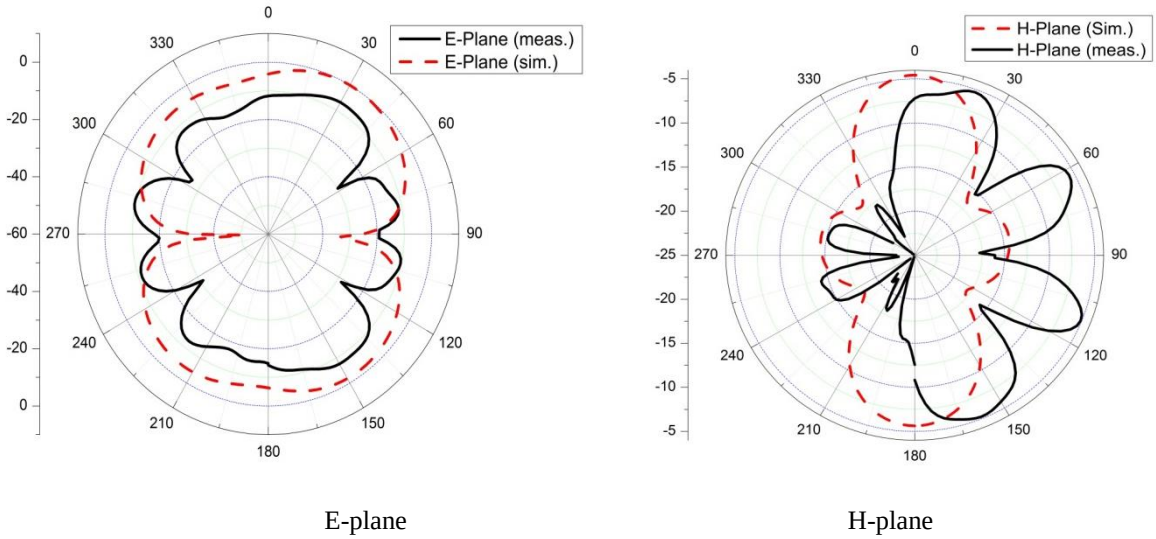

E-plane H-plane

(a)

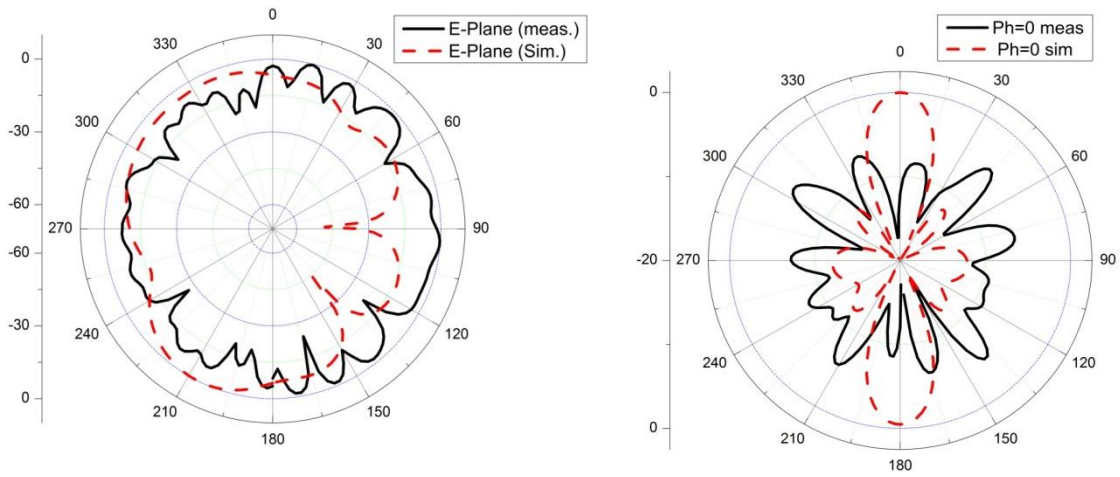

E-plane H-plane

(b)

Fig. 38. The measured and simulated far-field radiation pattern (E- plane and H-plane)

at: (a) f = 3.35 GHz (b) f = 7 GHz

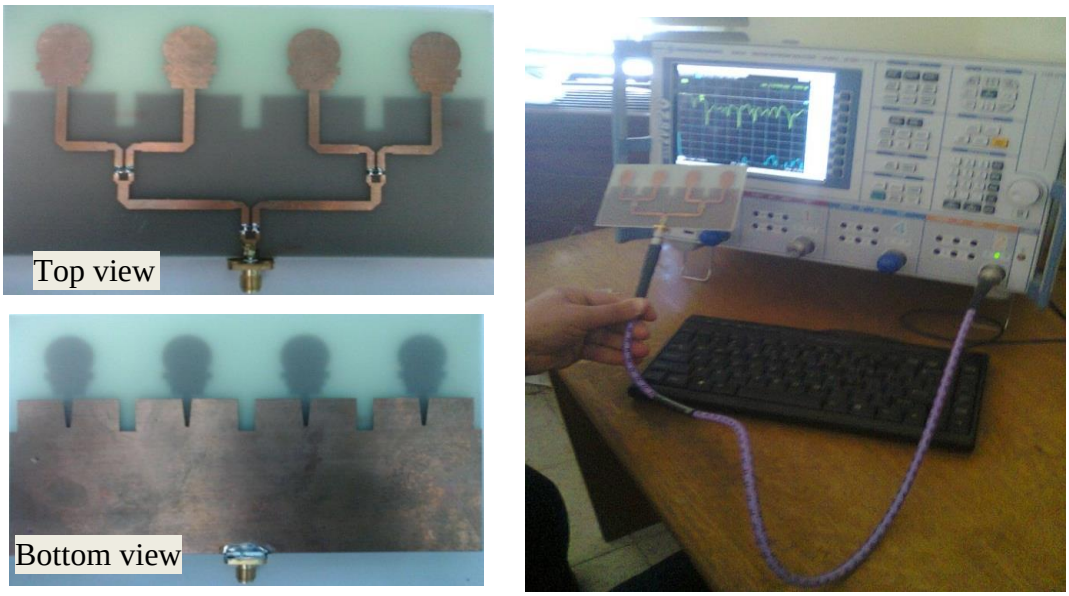

Fig. 39. The fabricated photos of the proposed 4 x1 UWB linear antenna array.

X. CONCLUSION

A novel and small UWB proposed monopole antenna with partial ground plane used for UWB communication systems has been investigated. A prototype with the optimal parameters and its electrical performance has been examined. The antenna demonstrates an ultra-wide impedance bandwidth prototype with satisfactory radiation patterns. An ultra-wideband antenna is operated with 3.1–12 GHz frequency range and size of 40×40 mm^2. In addition, a circuit modeling of UWB proposed antenna has been modeled. Moreover, a compatible lumped-elements used in the equivalent circuit modeling for the proposed monopole antenna is established using the Advanced Design System (ADS) software. A good agreement between the simulated return loss using CST- Microwave Studio and the return loss of the proposed equivalent circuit model for the proposed monopole antenna has been obtained. The simulated results of the proposed antenna satisfy the 10-dB return loss requirement for UWB as defined by the FCC. An UWB feeding network circuit has been designed / simulated in order to be used for exciting 2x1 and 4x1 linear antenna array. The simulated results for the proposed feed network has a good return loss, isolation and power division ratio at all ports within the whole UWB frequency range.

Two- and four-element UWB linear antenna arrays are presented. The average gain for the two-element antenna array is about 5.3 dBi and reaches to7.15 dBi for the four-element antenna array, over the whole UWB frequency range. A good agreement between the measured and the simulated results of four-element antenna array is appeared. In addition, the simulated radiation patterns of the antenna element and array are introduced.

REFERENCES

[1] Barrett, W. Terence, “History of Ultra Wideband Communications and Radar: Part I, UWB Communications", Microwave Journal, January 1st, 2001.

[2] FCC, “First report and order, revision of part 15 of the commission's rules regarding ultra-wideband transmission systems FCC," 2002.

[3] E. J. Wilkinson, “An N-way hybrid power divider,” IEEE Trans. Microw. Theory Tech., vol.8, No. 1, pp. 116-118, Jan. 1960.

[4] Ahmed, O. and A. R. Sebak, "A modified Wilkinson power divider/combiner for ultra-wideband communications," IEEE Antennas and Propagation Society International Symposium, 1-4, 2009.

[5] M. E. Bialkowski and A. M. Abbosh, “Design of a Compact UWB Out of-Phase Power Divider,” IEEE Microw. Wireless Compon. Lett., vol. 17, No. 4, pp. 289-291, Apr. 2007.

[6] Yang, L. and Q.-X. Chu, "Design of a compact UWB Wilkinson power divider," International Conference on Microwave and Millimeter Wave Technology (ICMMT), Vol. 1, 360-362, 2008.

[7] Lin, Z. and Q.-X. Chu, 'A novel compact UWB power divider for spatial power combining," Journal of Electromagnetic Waves and Applications, Vol. 23, No. 13, 1803-1812, 2009.
[8] CST Microwave Studio Electromagnetic Field Simulation Soft-ware, Computer Simulation Technology, Darmstadt, Germany. Progress In Electromagnetics Research C, Vol. 25, 2012.
[9] Zhou, B., H. Wang, and W.-X. Sheng, "A modified UWB Wilkin-son power divider using delta stub," Progress In Electromagnetics Research Letters, Vol. 19, pp 49-55, 2010.
[10] R. Pazoki, M. R. Ghafouri Fard and H. Ghafouri Fard, "A Modification in the Single-Stage Wilkinson Power Divider to Obtain Wider Bandwidth," Proc. Asia-Pacific Microw, Conf., pp. 2325-2328, Dec. 2007.
[11] X.-P. Ou and Q.-X. Chu, "A Modified Two-section UWB Wilkinson Power Divider", International Conference on Microwave and Millimeter Wave Technology (ICMMT) , China, vol.3, pp.1258-1260,April 21-29,2008.
[12] M. R. Ghaderi and F. Mohajeri," A compact hexagonal wide-slot antenna with microstrip-fed monopole for UWB application," IEEE antennas and wireless propagation letters, vol. 10, pp. 682-685,July 2011
[13] B. Gong, X. S. Ren, Y. Y. Zeng, L. H. Su, Q. R. Zheng," Compact slot antenna for ultra-wide band applications," IET, Microwaves Antennas & Propagation,vol. 8 , Issue 3 , pp.200-205, march 2014 .
[14] Yin, X.-C., C.-L. Ruan, C.-Y. Ding, and J.-H. Chu, "A planar U type monopole antenna for UWB applications," Progress In Electromagnetics Research Letters, Vol. 2, 1-10, 2008.
[15] Wang, H., H. Zhang, X. Liu, and K. Huang, "A CPW-FED ultra-wideband planar inverted cone antenna," Progress In Electromagnetics Research C, Vol. 12, 101-112, 2010.
[16] Kumar, M., A. Basu, and S. K. Koul, "UWB printed slot antenna with improved performance in time and frequency domains," Progress In Electromagnetics Research C, Vol. 18, 197-210, 2011.
[17] Li, P., J. Liang, X. Chen, and C. Parini, "A 4-element ultra-wideband tapered-slot-fed antenna array," IEEE Antennas and Propagation Society International Symposium, 4475-4478, Jul. 9-14, 2006.
[18] Y. Yang, Y. Wang, and A. E. Fathy, " Design of compact vivaldi antenna arrays for UWB see through wall applications," Progress In Electromagnetics Research, PIER 82, pp. 401–418, 2008
[19] Liao, C.-H., P. Hsu, and D.-C. Chang, "Side lobe control of UWB antenna array for real beam radar imaging," International Conference on Applications of Electromagnetism and Student Innovation Competition Awards (AEM2C 2010), 284-288, Aug. 2010.
[20] Chen, M. and J. Wang, "Planar UWB antenna array with CPW feeding network," Proceedings of Asia-Pacific Microwave Conference (APMC 2008),pp. 1-4, 2008.

AUTHOR BIOGRAPHIES

Mahmoud A. Mohanna Born 1946 in Egypt. Bachelor's degree in communication Engineering 1968, Cairo University. 20 years Radar specialist in Egyptian army forces. Microelectronics diploma 1986.Doctor of philosophy in communication engineering –microwave engineering 1994Tenured professor 2006 in National Research Institute of astronomy and geophysics Cairo.

Hosny A. Hosny El Metaafy Big boss of Computer Science Department Higher Technological Institute 10th of Ramadan city (H.T.I). Born 1951 in Egypt. Bachelor's degree in communication Engineering 1974, Military Technical College (M.T.C),Egyptian army forces.20 years Radar and Missile guidance specialist as instructor in (M.T.C) Egyptian army forces. Master in Microwave Engineering 1978Doctor of philosophy in electronic microwave engineering 1982.

El-Sayed Mostafa Kassem Assistant Instructor (Electrical and Computer Engineering Dept.) in Higher Technological Institute, tenth of Ramadan city, Cairo. M.Sc:- Electrical engineering (T V Image Processing) from Military Technical College, Cairo (1997). B.Sc:- Electrical engineering from Military Technical College, Cairo (1979) with grade EXCELLENT. ICDL certificate.